FORMATION CONDITIONS OF ICY MATERIALS IN COMET C/2004 Q2 (MACHHOLZ). I. MIXING RATIOS OF ORGANIC VOLATILES

Hitomi Kobayashi and Hideyo Kawakita
Department of Physics, Faculty of Science, Kyoto Sangyo University, Motoyama, Kamigamo, Kita-ku, Kyoto 603-8555, Japan; h_kobayashi@cc.kyoto-su.ac.jp

Abstract

We observed comet C/2004 Q2 (Machholz) with the Keck II telescope in late 2005 January and we obtained the spectra of C/2004 Q2 including many emission lines of volatile species such as H_2O, HCN, C_2H_2, NH_3, CH_4, C_2H_6, CH_3OH, and H_2CO with high-signal-to-noise ratios. Based on our observations, we determined the mixing ratios of the molecules relative to H_2O in C/2004 Q2. Since C/2004 Q2 is one of Oort Cloud comets, it is interesting to compare our results with other Oort Cloud comets. The mixing ratios of C_2H_2/H_2O and C_2H_6/H_2O in C/2004 Q2 are lower than typical Oort Cloud comets. Especially, C_2H_2/H_2O ratio in C/2004 Q2 is as lower as Jupiter Family comets. However, mixing ratios of other molecules in C/2004 Q2 are similar to typical Oort Cloud comets. C/2004 Q2 might be the intermediate type between Oort Cloud and Jupiter Family comets. To investigate the formation conditions of such intermediate type comet, we focused on the $(C_2H_2+C_2H_6)/H_2O$ ratios and $C_2H_6/(C_2H_6+C_2H_2)$ ratios in comets from the viewpoint of conversion from C_2H_2 to C_2H_6 in the precometary ices. We found that $(C_2H_2+C_2H_6)/H_2O$ ratio in C/2004 Q2 is lower than the ratio in typical Oort Cloud comets while $C_2H_6/(C_2H_6+C_2H_2)$ ratio in C/2004 Q2 is consistent with the ratio of the typical Oort Cloud comets and Jupiter family comets. If we assume that the cometary volatiles such as H_2O, CH_4, and C_2H_2 formed similar environment, the $C_2H_6/(C_2H_6+C_2H_2)$ ratio might not be sensitive in the temperature range where hydrogen-addition reactions occurred and cometesimals formed (∼30 K). We employed the dynamical-evolutional model and the chemical-evolutional model to determine the formation region of C/2004 Q2 more precisely. We found that comet C/2004 Q2 might have formed in relatively inner region of the solar nebula than the typical Oort Cloud comet (but slightly further than 5 AU from the proto-Sun).

Key words: comets: general – comets: individual (C/2004 Q2 Machholz) – solar system: formation

Online-only material: color figures, machine-readable table

1. INTRODUCTION

Comets are thought to be remnants of planetesimals formed in the solar nebula. Comets have clues to understand physical conditions (e.g., temperature, degree of ionization, dynamics of materials, and so on), and chemical evolution of materials in the solar nebula. From the viewpoint of the dynamics, comets are classified into two different dynamical groups by the Tisserand parameter with respect to Jupiter (T_J). These groups are called Near Isotropic Comets (NICs; $T_J < 2$) and Ecliptic Comets (ECs; $T_J > 2$). The latter also have a subgroup called Jupiter Family Comets (JFCs; $2 < T_J < 3$). NICs are further divided into two groups by the semimajor axis: long-period comets and Halley family comets (Duncan 2008). The dynamic origins of long-period comets and Halley family comets are thought to be Oort Cloud (Crovisier 2007; Duncan 2008), so we call these comets Oort Cloud comets (hereafter OCs).

Formation regions of these comets have been studied. Before 2005, it is thought that formation regions of OCs and JFCs are different from each other because of the differences in chemical compositions (e.g., A'Hearn et al. 1995). However, JFCs have relatively shorter orbital periods (typically several years) than OCs and it was concerned that the chemical compositions of icy materials on the surface of JFCs' nuclei have been changed by the solar heating effect. The NASA/Deep Impact experiment (A'Hearn et al. 2005) was conducted in 2005 to investigate the inner materials of comet 9P/Tempel 1, a JFC. The chemical composition of inner materials of 9P/Tempel 1 was similar to typical OCs (Mumma et al. 2005). Furthermore, fragmentation comet, 73P/Schwassmann-Wachmann 3 (hereafter SW3) was observed by various telescopes and instruments in 2006 (e.g.,

Schleicher, 2006; Kanda et al. 2008, in optical; Villanueva et al. 2006; Dello Russo et al. 2007; Kobayashi et al. 2007, in near-infrared; Lis et al. 2008; Biver et al. 2008, in radio). From the near-infrared observations, the chemical compositions of the fragments "B" and "C" of SW3-B were similar to C/1999 S4 (LINEAR) (Mumma et al. 2001a; Dello Russo et al. 2007; Kobayashi et al. 2007). C/1999 S4 is an OC but peculiar in chemistry (depleted in organics) compared with other OCs. Therefore, the formation regions of both OCs and JFCs might be partly overlapped in the solar nebula. On the other hand, there are many dynamical simulations of planetesimals which are origin of comets. One of the reliable dynamical models is the "Nice model" (Morbidelli et al. 2008). This model can explain many things simultaneously (orbital parameters of giant planets and Trans Neptunian Objects (TNOs), migrations of giant planets in the solar nebula, origin of the late heavy bombardment, and so on). According to this model, the formation regions of comets are: (1) 16–30 AU in the solar nebula for the JFCs; (2) Jupiter–Saturn region (5–15 AU); and (3) 16–30 AU in the solar nebula for the OCs. From the viewpoint of dynamics, both JFCs and a part of OCs have the common formation region. However, formation regions of OCs are widely expanded in the solar nebula (5–30 AU). Since it is difficult to specify the formation region of an OC from the dynamical properties only, observations to reveal the chemistry of the OC are essentially important. Especially, to investigate the population distribution of OCs that formed in different regions, we need to observe many OCs and to determine chemical compositions of the comets.

In this paper (Paper I), we present high dispersion spectra of comet C/2004 Q2 (Machholz) in near-infrared region and

we report the mixing ratios of organic volatiles in the comet. C/2004 Q2 is an Oort Cloud comet discovered in 2004 August, and the comet is thought to be a dynamically new comet (Marsden, 2004; Levison, 1996). Our scientific goal is to investigate the formation conditions of icy materials that formed C/2004 Q2 based on the mixing ratios of organics. Deuterium-to-hydrogen ratios (D/H ratios) and nuclear spin isomers' ratios are also the useful tools to investigate the formation conditions of icy materials. We also investigated the D/H ratio of CH_4 and nuclear spin isomers' ratios of CH_4 and H_2O in this comet (Kawakita & Kobayashi 2009, hereafter Paper II). The results on the D/H ratio and nuclear spin isomers in comet C/2004 Q2 indicate that comets might form in relatively warmer regions than typical Oort Cloud comets. We compare the conclusion in Paper II with that based on the mixing ratios of organic molecules shown in this paper (this comparison will help us to understand the cosmogonic meaning of the D/H ratios and nuclear spin isomers' ratios in comets).

2. OBSERVATION AND DATA ANALYSIS

High-resolution spectroscopic observations of comet C/2004 Q2 (Machholz) in near-infrared (the *L* band) were performed on 2005 January 30, using the Keck II 10 m telescope with the NIRSPEC (McLean et al. 1998) located atop Mauna Kea, Hawaii. In the *L*-band region, we can cover rovibrational bands of some organic molecules (e.g., H_2O, OH, HCN, C_2H_2, CH_4, CH_3OH, and H_2CO). The NIRSPEC has the cross-dispersed echelle spectroscopy mode, and it can achieve high resolving power ($\lambda/\Delta\lambda \sim 25,000$ with the slit size of $0''.43$ by $24''$). We used this mode for our observations. In late 2005 January, C/2004 Q2 became as bright as about fourth magnitude in *V* band and heliocentric distance, geocentric distance, and geocentric velocity were 1.21 AU, 0.48 AU, and +15.6 km s^{-1} at the observations, respectively. A photometric standard star (HR937; spectral type is G0V) was observed for flux calibration. The telescope was nodded by $12''$ along the slit such that the comet remained in the slit for both A and B positions. The observations were acquired in the sequence A − B − B − A. We obtained nine ABBA sequences for the comet and total integration time on the comet was 2160 s. The total integration time for the standard star was 20 s for one ABBA sequence.
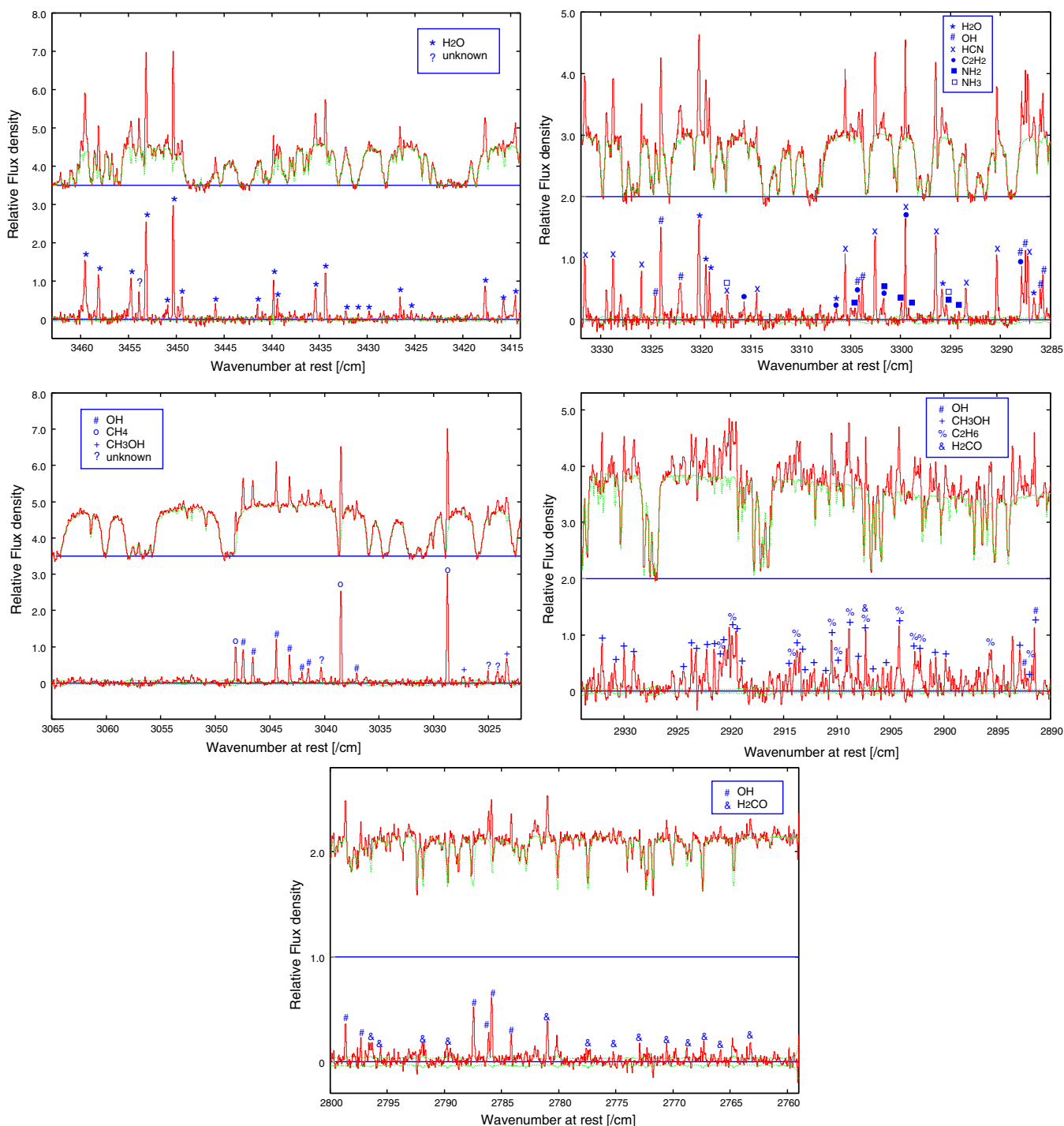
Obtained data were reduced using Image Reduction and Analysis Facility (IRAF) software package provided by National Optical Astronomy Observatory (NOAO). For each sequence of ABBA, we calculated 2A–2B (A − B − B + A) to subtract the background sky emission and the results were flat-fielded. These data contain six echelle orders (21st ∼ 26th orders) at once. After each echelle order was extracted as a strip image, the strip was rectified and wavelength-calibrated. The known positions of sky background emission lines enabled wavelength calibration of the data. The cometary spectra centered on the nucleus were extracted from the area corresponding to 9 pixel rows ($1''.8$ at the sky) along the slit and flux-calibrated by using the spectra of photometric standard star. The modeled telluric absorption spectra were produced by the LBLRTM code (Clough et al. 2005) based on the HITRAN 2004 database (Rothman et al. 2005). Emission lines were obtained by subtracting the reflected sunlight by cometary dust grains. For more detailed information about data reduction, refer to Kobayashi et al. (2007). Figure 1 shows the selected spectra which contain emission lines from H_2O, OH, HCN, C_2H_2, NH_2, NH_3, CH_4, C_2H_6, CH_3OH, and H_2CO.

3. RESULTS

A rotational temperature (T_{rot}) is necessary to determine the emission efficiencies (*g*-factors) of individual rovibrational molecular lines. We determined T_{rot} for H_2O and HCN from our observations. In the case of H_2O, we constructed the fluorescence excitation model based on Dello Russo et al. (2004, 2005). In this model, H_2O molecules are pumped from the ground vibrational state to the upper vibrational states by the solar radiation field. The population distributions among rotational levels in the ground vibrational state are described by a Boltzmann distribution at a given rotational temperature. We used the solar radiation field provided by Kurucz (2005) for optical and the modeled solar spectrum for near-infrared (Kurucz 1994). When we construct the H_2O fluorescence excitation model, the ortho-to-para abundance ratio (OPR) is an important parameter. The ortho- and para-H_2O are distinguished by a total nuclear spin quantum number (*I*); $I = 1$ (two nuclear spins of H atoms are in parallel) for ortho-H_2O and $I = 0$ (two nuclear spins of H atoms are in anti-parallel) for para-H_2O. The high-temperature limit of the OPR of H_2O is 3.0 (nuclear spin statistical weight ratio). Bonev et al. (2007) reported that OPR of H_2O in C/2004 Q2 is 2.86 ± 0.17 (this error corresponds to systematic uncertainty).[1] We adopted this OPR to determine the rotational temperature of H_2O. The T_{rot} of H_2O is determined by using the rotational temperature analysis as follows (Dello Russo et al. 2004). The ratio of line fluxes to corresponding *g*-factor (F/g) that vary with T_{rot} should be constant regardless of the wide range of upper state rotational energies if we take the correct rotational temperature for the ground vibrational levels. We plot the F/g versus upper state rotational energy (E′–E′ (lowest)) and determine the rotational temperature for which the slope of the straight line for F/g versus (E′–E′ (lowest)) is horizontal (see Figure 2(a) for H_2O). The T_{rot} of H_2O is determined as (83 ± 4) K from this analysis. In the case of HCN, we constructed the fluorescence excitation model based on Magee-Sauer et al. (1999). In this model, HCN molecules are pumped from the ground vibrational state to the upper vibrational state by the solar radiation field same as H_2O. We assumed that the population distribution among rotational levels in the vibrational ground state followed the Boltzmann distribution at a given rotational temperature. The T_{rot} of HCN is determined as (78 ± 4) K from the similar analysis as that of H_2O (the result of rotational temperature analysis of HCN is shown in Figure 2(b)). Both results of T_{rot} for H_2O and HCN are consistent within their error bars. This fact suggests that the rotational excitation of these molecules was controlled by intermolecular collisions in the inner coma, so these molecules were thermalized well.

We modeled the fluorescence excitation of C_2H_2 in the same manner as HCN. In our spectrum, we can find six rovibrational emission lines of the C_2H_2 ν_3-vibrational band (see Figure 1). Some of these emission lines are contaminated with other molecular emission lines. For instance, the R4 of C_2H_2 is blended with H_2O (3306.40 cm^{-1}, (200)2_{02}–(001)3_{21}; see Table 1); the R3, P3, and P4 lines are blended with OH; the R2 is blended with NH_2; and the R1 is blended with HCN. For the R4 line, we removed the contamination by using flux and

---

[1] Recently Kawakita & Kobayashi (2009, Paper II) found the OPR of water in C/2004 Q2 to be 3.13 (+0.56/−0.42) that is also consistent with high-temperature limit (3.0). It is also consistent with the value reported by Bonev et al. (2007). The derived water production rates (and mixing rates) for both OPRs are not so different. If we use OPR = 3.0, the derived Q(H_2O) is smaller by about 3% than the case of OPR = 2.86.

Figure 1. Selected spectra of H_2O, OH, HCN, C_2H_2, NH_3, CH_4, C_2H_6, CH_3OH, and H_2CO in C/2004 Q2 (Maccholz) on 2005 January 30.
(A color version of this figure is available in the online journal.)

g-factors of blended molecular emission lines with these C_2H_2 lines, as follows. First we estimate the line flux of blended H_2O with C_2H_2 (F_{H2O}) based on the line flux of nearby emission lines of H_2O at 3319.47 cm^{-1} and 3319.12 cm^{-1} (F'_{H2O}; their summation, see Table 1). The ratio of F_{H2O} and F'_{H2O} should be the same as the ratio of corresponding g-factors. After we estimate F_{H2O}, we subtract it from the flux of blended line (C_2H_2+H_2O) to obtain the line flux of C_2H_2 only. For R3, we neglect the contamination from OH because the vibrational quantum number of the blended OH is high (transition from
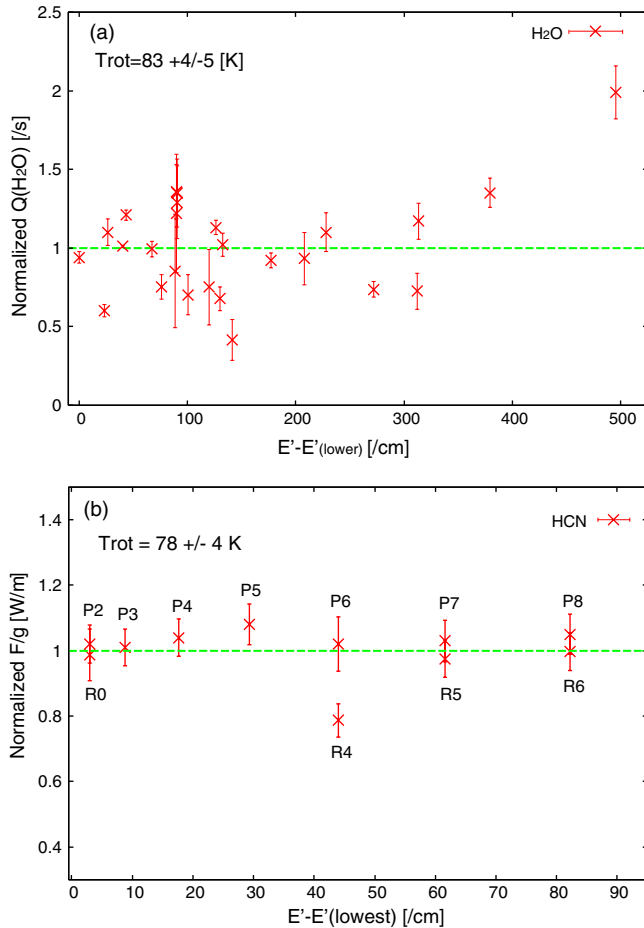
$v' = 3$ to $v'' = 2$) and Einstein's A-coefficient is relatively small. Such high-v' OH line has never been observed in comet. Since other C_2H_2 lines (R2, R1, P3, and P4) could not be de-blended from the blended emissions, we used only two C_2H_2 lines (R4 and R3) to determine the mixing ratio. We assumed that T_{rot} of C_2H_2 is 80 K (almost the same as T_{rot} of H_2O and HCN) and that the nuclear spin isomers ratio is 3 (high-temperature limit) for C_2H_2.

We modeled the fluorescence excitation of CH_4 based on Gibb et al. (2003). We detected three CH_4 lines (R2, R1, R0

Table 1
Line Fluxes and g-Factors including Transmittances.

H_2O								
Line assignment Upper state–Lower state		Wavenumber (cm^{-1})	Flux (W m^{-2})			g-factor (W s^{-1})		
$(v_1, v_2, v_3) J_{Ka\,Kc}$	$(v_1, v_2, v_3) J_{Ka\,Kc}$	(rest)	Set 1	Set 2	Set 3	Set 1	Set 2	Set 3
$(2, 0, 0) 2_{1\,1}$	$(0, 0, 1) 2_{1\,2}$	3459.63	1.64E-18	1.05E-18	1.16E-18	2.25E-27	2.15E-27	2.00E-27
$(1, 0, 1) 1_{1\,1}$	$(0, 0, 1) 2_{0\,2}$	3459.53						
$(1, 0, 1) 4_{3\,1}$	$(1, 0, 0) 5_{3\,2}$	3459.49						
$(1, 0, 1) 4_{4\,1}$	$(0, 0, 1) 5_{3\,2}$	3459.49						
$(2, 0, 0) 4_{3\,2}$	$(1, 0, 0) 4_{3\,2}$	3458.52	1.16E-19	1.10E-19	7.31E-20	1.12E-28	1.05E-28	9.47E-29
$(1, 0, 1) 0_{0\,0}$	$(0, 0, 1) 1_{1\,1}$	3458.12	7.64E-19	7.10E-19	7.94E-19	1.65E-27	1.47E-27	1.22E-27
$(1, 0, 1) 3_{0\,3}$	$(0, 0, 1) 3_{1\,2}$	3455.43	1.62E-19	8.57E-20	1.99E-19	3.13E-28	2.96E-28	2.71E-29
$(1, 1, 1) 1_{0\,1}$	$(0, 1, 1) 1_{1\,0}$	3454.87	8.36E-19	9.95E-19	8.11E-19	1.31E-27	1.27E-27	1.21E-27
$(1, 0, 1) 2_{1\,1}$	$(0, 0, 1) 2_{2\,0}$	3454.69						
$(2, 0, 0) 1_{1\,0}$	$(1, 0, 0) 2_{2\,1}$	3453.3	1.46E-18	1.29E-18	1.55E-18	3.07E-27	2.89E-27	2.66E-27
$(1, 0, 1) 2_{0\,2}$	$(1, 0, 0) 3_{2\,1}$	3453.15						
$(1, 0, 1) 4_{1\,3}$	$(0, 0, 1) 4_{2\,2}$	3451.09	1.58E-19	1.79E-19	8.40E-20	3.08E-28	2.97E-28	2.81E-28
$(2, 0, 0) 5_{2\,4}$	$(1, 0, 0) 5_{3\,3}$	3451.02						
$(1, 0, 1) 3_{1\,3}$	$(1, 0, 0) 3_{3\,0}$	3450.9	1.00E-18	1.71E-19	3.09E-19	4.89E-28	4.70E-28	4.41E-28
$(2, 0, 1) 2_{1\,2}$	$(2, 0, 0) 1_{1\,1}$	3450.82						
$(2, 0, 0) 5_{1\,5}$	$(1, 0, 0) 5_{2\,4}$	3450.78						

(This table is available in its entirety in a machine-readable form in the online journal. A portion is shown here for guidance regarding its form and content.)

Figure 2. F/g vs. upper state rotational energy of H_2O (a) and HCN (b). The g-factor has a dependence on rotational temperature (T_{rot}). The optimum T_{rot} of H_2O and HCN in C/2004 Q2 (Machholz) is 83 (±4) and 78 (±4) K, respectively. Both T_{rot} of H_2O and HCN are consistent within the error bars.
(A color version of this figure is available in the online journal.)

of v_3 band) in our spectra. However, we eliminated R2 line because of poor transmittance at the line position. We used only two lines for determining the mixing ratio. We assumed T_{rot} of 80 K for CH_4 as same as C_2H_2. The nuclear spin isomers' ratios are also assumed to be high-temperature limits (A:E:F = 5:2:9) for CH_4.

In the case of C_2H_6 and CH_3OH, the v_7 Q-branch of C_2H_6 (~3000 cm^{-1}) and the v_3 Q-branch of CH_3OH (~2844 cm^{-1}) are usually used to determine rotational temperatures or production rates of these molecules in the high-dispersion spectroscopic observations of comets in the near-infrared region. However, we detected emission lines from C_2H_6 and CH_3OH around 2890–2934 cm^{-1} in our observations and neither the CH_3OH v_3 Q-branch nor the C_2H_6 v_7 Q-branch is detected. A part of these emission lines around 2890–2934 cm^{-1} were identified as the v_5 band of C_2H_6 (Dello Russo et al. 2006, 2008) while vibrational and rotational assignments of the CH_3OH lines were not determined (Dello Russo et al. 2006). Fortunately, Dello Russo et al. (2008) reported the g-factor of the v_5 $^QP_3$ line of C_2H_6 for $T_{rot} = 79$ K in the case of comet 17P/Holmes and we detected the same line in C/2004 Q2. This T_{rot} assumed in 17P/Holmes is similar to the rotational temperatures determined for H_2O and HCN in C/2004 Q2 (~80 K). Therefore, we adapted the g-factor of C_2H_6 at 79 K to our observations. For CH_3OH, a g-factor of the CH_3OH v_3 Q-branch is only available ($g = 2.17 \times 10^{-5}$ s^{-1}: Dello Russo et al. 2008, 2006; Brooke et al. 2003; Bockelée-Morvan et al. 1995) and there is no report for the g-factors of CH_3OH lines around 2890–2934 cm^{-1}. Dello Russo et al. (2006) reported the line intensities of both the CH_3OH v_3 Q-branch lines and the CH_3OH lines around 2890–2934 cm^{-1} in comet C/1999 H1 (Lee). Since both comet Lee and C/2004 Q2 had similar T_{rot} for other molecules (70–80 K for Lee, ~80 K for C/2004 Q2) and the g-factors of total v_3 Q-branch is not sensitive to the rotational temperature (of course, each line is sensitive to the rotational temperature, but whole Q-branch is not sensitive), we determined the g-factors of individual CH_3OH emission lines around 2890–2934 cm^{-1} based on the ratios of

Table 2
Mixing Ratios of C/2004 Q2 (Machholz).[a]

Molecule	T_{rot} (K)	Production Rate (s^{-1})	Mixing ratio (%)	Remarks
H_2O	83 ± 4	$(3.42 \pm 0.19) \times 10^{29}$	...	27 lines
HCN	78 ± 4	$(5.53 \pm 0.38) \times 10^{26}$	0.16 ± 0.01	11 lines in ν_3 band
C_2H_6	(79)	$(1.46 \pm 0.20) \times 10^{27}$	0.43 ± 0.06	ν_5 $^qP_3$
C_2H_2	(80)	$(1.94 \pm 0.14) \times 10^{26}$	0.057 ± 0.004	ν_3 R3, R4
CH_4	(80)	$(3.43 \pm 0.19) \times 10^{27}$	1.0 ± 0.1	ν_3 R0, R1
CH_3OH	(70–80)	$(4.01 \pm 0.21) \times 10^{27}$	1.2 ± 0.1	4 lines
H_2CO	(80)	$(6.06 \pm 0.46) \times 10^{26}$	0.18 ± 0.01	18 lines in ν_1 and ν_5 bands
NH_3	(80)	$(1.08 \pm 0.48) \times 10^{27}$	0.32 ± 0.05	ν_1 a^{q}P(2, 1) + a^{q}P(2, 0)

Note. [a] Error bars correspond to $\pm 1\sigma$.

line intensities relative to the total intensity of ν_3 Q-branch are listed in Dello Russo et al. (2006). Here, we assumed that no unknown emission lines contaminate the ν_3 Q-branch and the unassigned lines of CH_3OH around 2890–2934 cm^{-1} listed in Dello Russo et al. (2006).

We also detected some H_2CO lines and one NH_3 emission line. We adapted a T_{rot} of 80 K to those molecules. In the case of H_2CO, we used g-factors listed in Reuter et al. (1989). In the case of NH_3, we established the fluorescence excitation model as we did for HCN and C_2H_2 (NH_3 is pumped from the ground vibrational state to the upper vibrational state by the solar radiation field, the population distribution among rotational levels in the vibrational ground state followed a Boltzmann distribution at a given rotational temperature). Since the detected NH_3 line is contaminated by NH_2 line (ν_3-band 1_{11}–1_{10}, $\sim$ 3295.4 cm^{-1}), we removed the contamination of NH_3 based on multiple measurements of NH_2 lines and g-factors of NH_2 (the blended NH_2 line with this NH_3 is included in) as in the case of C_2H_2 (+ H_2O).

Finally, we derived the mixing ratios of some molecules with respect to H_2O in C/2004 Q2. The mixing ratio was obtained by comparing production rates of some molecular species with that of water. We can estimate the gas production rate, Q, as follows:

$$Q = \frac{4\pi\Delta^2}{f_{geom}\tau} \frac{F}{g} [\text{mol s}^{-1}],$$

where Δ denotes the geocentric distance (m), f_{geom} denotes the fraction of considered molecules within the observed (slit) aperture, τ denotes the lifetime of the molecule (s) (Huebner et al. 1992), F denotes the observed line flux at the top of the atmosphere [J m^{-2} s^{-1}], and g denotes the g-factor of the observed line (J s^{-1} molecule^{-1}). In the above formula, τ, F, and g have a molecular dependence, however, f_{geom} is proportional to τ^{-1} in the inner coma (where the traveling time of molecules from the nucleus is much shorter than the photodissociation time), and τ is canceled by f_{geom} (Kobayashi et al. 2007). Thus, the gas production rate is proportional to F/g and the ratio of Qs is almost equal to the F/g ratio. Fluxes and g-factors used to determine the T_{rot} and mixing ratios are listed in Table 1, and the mixing ratios of C/2004 Q2 are listed in Table 2.

The 1σ error levels of mixing ratios in C/2004 Q2 are estimated as follows. The nine ABBA sequences were divided in three sets (1st–3rd seq. for set no.1, 4th–6th seq. for set no.2, and 7th–9th seq. for set no. 3) and these three sets were reduced separately. Flux was measured in each set. We used the standard deviation of the measurements for three sets as the error of each line flux. Thus, the error levels estimated here contain both the stochastic noise (mainly originated in sky

background) and the errors originated from the determination of atmospheric transmission as well as the difference in the slit loss. The differences in the slit loss of cometary fluxes for these three sets were corrected by comparing total flux (gas emission + dust continuum) within the wide wavelength range in each set (we determined the ratios of the total flux of set no.1:total flux of set no.2:total flux of set no.3 and scaled them by these ratios). The errors obtained here are slightly higher than the stochastic noise estimated from the sky background emission only based on the photon statistics.

4. DISCUSSIONS

We compared the mixing ratios obtained by us with results of Bonev et al. (2009) and Biver et al. (2005) in Table 3. The trend of mixing ratios is almost consistent with one another. Precisely, however, there are small differences in some molecular species. For example, in the case of C_2H_6, the mixing ratio obtained from our observations is lower than that listed in Bonev et al. (2009). This difference is probably caused by the difference in used lines (they used lines in the ν_7 band while we used the line in the ν_5 band). In the cases of C_2H_2 and CH_4, situations are similar to that of C_2H_6. In the case of H_2CO, the mixing ratio obtained in this study is higher than that listed in Bonev et al. (2009). They used only a single composite line of the ν_1-band Q-branch although we used multiple lines including the composite of the ν_1-band Q-branch. In the case of CH_3OH, we used different g-factors and different lines. If we determine the mixing ratio based on the same g-factor (ν_3-band Q-branch) used by Bonev et al. (about half of ours, M. A. DiSanti 2008, private communication), the mixing ratios are almost consistent with each other. Radio observations (Biver et al. 2005) also showed a similar mixing ratio of CH_3OH, $\sim$2.5 (%).

We also compared mixing ratios of C/2004 Q2 with mixing ratios of other comets (both OCs and JFCs) obtained by the previous studies. The mixing ratios of such comets listed in DiSanti & Mumma (2008) are summarized in Table 3. We found that C/2004 Q2 was strongly depleted in C_2H_X molecules compared with the typical OCs. Particularly, the mixing ratio of C_2H_2 in C/2004 Q2 is as low as JFCs. However, mixing ratios of other molecules such as CH_4 and HCN are consistent with other OCs. The mixing ratio of CH_3OH is almost half of typical OCs because DiSanti & Mumma (2008) used a different g-factor for CH_3OH from ours. They used ν_3 Q-branch g-factor of CH_3OH that is almost half compared with ours (M. A. DiSanti 2008, private communication), as discussed above. Unfortunately, we are still in need of a complete theory of the CH_3OH vibrational spectrum that can explain individual line strengths in near-infrared. Sometimes CH_3OH mixing ratios coming from different kinds of observations and modeling

Table 3
Comparison Between C/2004 Q2 and Other Comets.[a]

Comet	HCN	C_2H_6	C_2H_2	CH_4	CH_3OH	H_2CO	NH_3	Remarks [b]
C/2004 Q2	0.16 ± 0.01	0.43 ± 0.06	0.057 ± 0.004	1.0 ± 0.1	1.2 ± 0.1	0.18 ± 0.01	0.32 ± 0.05	This work
C/2004 Q2	$0.15^{+0.01}_{0.02}$	0.56 ± 0.02	0.09 ± 0.01	1.46 ± 0.08	2.14 ± 0.12	0.11 ± 0.03	0.37 ± 0.06	1
C/2004 Q2	0.1	. . .	. . .	. . .	2.5	. . .	. . .	2
Typical OCs	0.2–0.3	0.6	0.2–0.3	0.5–1.5	2	. . .	. . .	3
C/1996 B2	0.18 ± 0.04	0.62 ± 0.07	0.16 ± 0.08	0.79 ± 0.08	1.7 ± 0.4	. . .	. . .	4
C/1995 O1	0.27 ± 0.04	0.56 ± 0.04	0.31 ± 0.1	1.45 ± 0.16	2.4 ± 0.3	. . .	. . .	5
C/1999 H1	0.29 ± 0.02	0.67 ± 0.07	0.27 ± 0.03	1.45 ± 0.18	2.1 ± 0.5	. . .	. . .	6
153P/I-Z	0.18 ± 0.05	0.62 ± 0.18	0.18 ± 0.05	0.51 ± 0.06	2.5 ± 0.5	. . .	. . .	7
C/2001 A2	0.6 ± 0.1	1.7 ± 0.2	0.5 ± 0.1	1.2 ± 0.2	3.9 ± 0.4	. . .	. . .	8
1P/Halley	~ 0.2	~ 0.4	~ 0.3	< 1	1.7 ± 0.4	. . .	. . .	9
C/1999 S4	0.10 ± 0.03	0.11 ± 0.02	$< 0.12^a$	0.18 ± 0.06	< 0.15	. . .	. . .	10
9P/Tempel 1	0.22 ± 0.03	0.40 ± 0.04	0.13 ± 0.04	0.54 ± 0.3	0.99 ± 0.17	. . .	. . .	11, Post impact
73P/SW3-B	0.28 ± 0.02	0.16 ± 0.02	0.03 ± 0.01	. . .	0.20 ± 0.03	0.14 ± 0.02	< 0.16	12, 2006 May 14.6
73P/SW3-C	0.24 ± 0.01	0.11 ± 0.01	0.05 ± 0.02	. . .	0.15 ± 0.03	0.15 ± 0.03	< 0.33	12, 2006 May 14.6

Notes.
[a] Error bars correspond to $\pm 1\sigma$. The upper limits correspond to 3σ.
[b] 1: Bonev et al. (2009), weighted mean of 2004 November 28 & 2005 January 19.
C_2H_2 and NH_3 were obtained on January 19 only (we referred the results at $T_{rot} = 93$ K).
2: Biver et al. (2005), radio observation.
3: Mumma et al. (2003).
4: HCN : Magee-Sauer et al. (2002a).
C_2H_6 : Eberhardt et al. (1994), Dello Russo et al. (2002a).
C_2H_2 : Magee-Sauer et al. (2001).
CH_4 : Gibb et al. (2003), Mumma et al. (1996).
CH_3OH : Biver et al. (1999a).
5: HCN, C_2H_2 : Magee-Sauer et al. (2001).
C_2H_6 : Dello Russo et al. (2001).
CH_4 : Gibb et al. (2003), Weaver et al. (1999).
CH_3OH : Biver et al. (1999b).
6: HCN, C_2H_6, C_2H_2, CH_3OH : Mumma et al. (2001a).
CH_4 : Gibb et al. (2003), Weaver et al. (1999).
7: HCN, C_2H_2 : Magee-Sauer et al. (2002b).
C_2H_6 : Dello Russo et al. (2002b).
CH_4 : Gibb et al. (2003).
CH_3OH : DiSanti et al. (2002).
8: HCN, C_2H_6, C_2H_2, CH_3OH : Magee-Sauer et al. (2008).
CH_4 : Gibb et al. (2007).
9: HCN : Bockelée-Morvan et al. (1987), Schloerb et al. (1986), Despois et al. (1986).
C_2H_6, CH_4, C_2H_2 : Eberhardt (1999).
CH_3OH : Eberhardt et al. (1994).
10: HCN, C_2H_6, C_2H_2, CH_3OH : Mumma et al. (2001b).
CH_4 : Gibb et al. (2003), Mumma et al. (2001b).
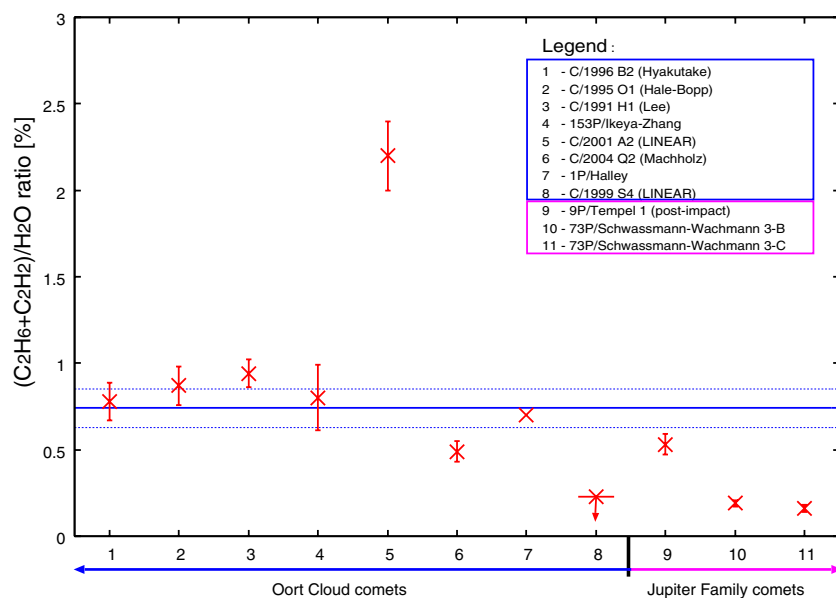11: HCN, C_2H_6 : DiSanti et al. (2007).
CH_4, C_2H_2, CH_3OH : Mumma et al. (2005).
12: Dello Russo et al. (2007).

are inconsistent among them. Such discrepancy is probably caused by the fact that most lines are not well identified in near-infrared, and there is little knowledge about Einstein's A-coefficients for the ν_3 band of CH_3OH (see Brooke et al. 2003). Future investigations of excitation models of CH_3OH in near-infrared are strongly recommended. If we use the same g-factor of CH_3OH ν_3 Q-branch as DiSanti & Mumma (2008), the mixing ratio of CH_3OH is almost same with other OCs (if we use the g-factor used by DiSanti & Mumma (2008), mixing ratio of CH_3OH in C/2004 Q2 would be 2.65 ± 0.14 (%)). We can conclude that the mixing ratio of CH_3OH in C/2004 Q2 is consistent with other OCs. Because C/2004 Q2 is a long periodic comet, this comet might preserve more primordial materials than JFCs (note that the fragments of comet 73P/SW3 were exceptions since it showed fragmentation events and the fresh materials were exposed on their surfaces).

The depletion in C_2H_X relative to H_2O in C/2004 Q2 is thought to be intrinsic (not caused by the solar heating effect during many passages around the Sun). These facts might suggest that C/2004 Q2 is the intermediate type between OCs and JFCs.

How did such intermediate type comets form in the solar nebula? We have to investigate the origin of planetesimals that consist of comets in the solar nebula. If the cometary nuclei are heterogeneous in chemistry, it is considered that the cometary nuclei are aggregates of planetesimals formed in various regions in the solar nebula. There might be some mechanisms to mix planetesimals in the solar nebula. The homogeneity of cometary nucleus are studied in 9P/Tempel 1 (by the NASA/Deep Impact experiment), C/2001 A2 (LINEAR), a comet pair of C/1988 A1 (Liller) and C/1996 Q1 (Tabur), and 73P/SW3 (fragments B and C). In the case of a comet pair of comet Liller and comet

Figure 3. $(C_2H_6+C_2H_2)/H_2O$ ratios in comets listed in Table 4. If C_2H_6 was formed by hydrogen-addition reaction to C_2H_2 on cold grain, mixing ratio of C_2H_6 is related to original quantity of C_2H_2 and conversion efficiency from C_2H_2 to C_2H_6. The former is related to $(C_2H_6+C_2H_2)/H_2O$ (the latter related to $C_2H_6/(C_2H_6+C_2H_2)$ ratios; see Figure 4). If the original quantity of C_2H_2 was depleted, the ratio should show the lower value. The solid line shows the averaged value of $(C_2H_6+C_2H_2)/H_2O$ ratio and dashed lines indicate $\pm3\sigma$ error bars of averaged value. The $(C_2H_6+C_2H_2)/H_2O$ ratio of C/2004 Q2 shows lower than averaged value of that of other comets. This fact suggests the formation region of C/2004 Q2 depleted in C_2H_2 than the forming regions of other OCs.
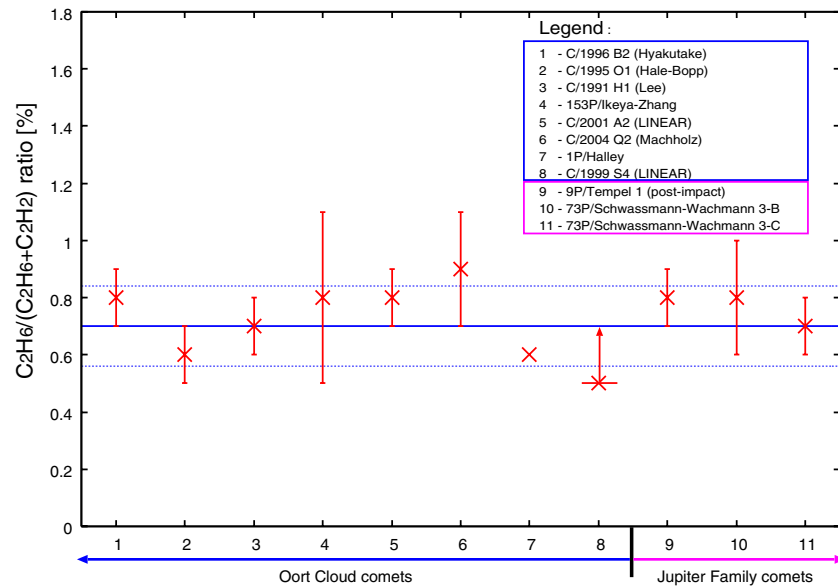(A color version of this figure is available in the online journal.)

Tabur, and in the case of SW3-B and -C fragments, these comets are fragmentation comets and it is thought that the fresh ices in the interior of cometary nuclei were exposed. Their parent nuclei are thought to be homogeneous in chemistry (Turner & Smith 1999; Dello Russo et al. 2007; Kobayashi et al. 2007). In contrast, the nuclei of C/2001 A2 and 9P/Tempel 1 might be heterogeneous in chemistry as reported by Gibb et al. (2007) and Feaga et al. (2007), respectively. However, it is difficult to conclude that the heterogeneity in the nuclei of both C/2001 A2 and 9P/Tempel 1 is natural. Such heterogeneity might exist only near the surface of the nucleus due to solar heating effect. Here, we assumed that the nucleus of C/2004 Q2 was homogeneous in the discussions below since there is no report about the heterogeneity in C/2004 Q2.

The nucleus of C/2004 Q2 could be considered as homogeneous, in other words, the formation regions of planetesimals were chemically similar regions or environments in the solar nebula. We discuss on such special regions or environment (C_2H_2 and C_2H_6 were depleted and other molecules were normal) in the solar nebula in order to explain the mixing ratios of C/2004 Q2. Here, we assumed that C_2H_2 is the parent species in the comet based on its spatial distribution in the coma, that is, C_2H_2 was included in the cometary nucleus as ice and sublimated from the nucleus directly. If C_2H_6 was made from C_2H_2 by hydrogen-addition reactions on the grain surface in the solar nebula (Villanueva et al. 2006 and references therein), the mixing ratio of C_2H_6 depends on the original quantity of C_2H_2 and the conversion efficiency from C_2H_2 to C_2H_6. We compared $(C_2H_2+C_2H_6)/H_2O$ ratio in C/2004 Q2 with other comets to estimate the original quantity of C_2H_2. Figure 3 shows $(C_2H_2+C_2H_6)/H_2O$ ratios in comets listed in DiSanti & Mumma (2008) and C/2004 Q2. The $(C_2H_2+C_2H_6)/H_2O$ ratio in C/2004 Q2 is lower than typical OCs. This result implies the forming region of C/2004 Q2 initially depleted in C_2H_2 than the forming regions of other OCs. In this figure, we can also find the group depleted in $(C_2H_2+C_2H_6)$, e.g., C/1999 S4 (LINEAR),

9P/Tempel 1, and 73P/SW3. These comets are also depleted in C_2 (aka, C_2-depleted comets; A'Hearn et al. 1995) in optical observations (Fink 2009; Farnham et al. 2001; Kanda et al. 2008). Although the depletion in C_2 probably correlated to the depletion in $(C_2H_2+C_2H_6)$, we need more number of samples for the statistical investigation.

Furthermore, we focused on $C_2H_6/(C_2H_6+C_2H_2)$ ratio that is an indicator of the conversion efficiency from C_2H_2 to C_2H_6 and these results are shown in Figure 4. The $(C_2H_2+C_2H_6)/H_2O$ and $C_2H_6/(C_2H_6+C_2H_2)$ ratios are listed in Table 4. In Figure 4 and Table 4, we can find that $C_2H_6/(C_2H_6+C_2H_2)$ ratios of all OCs and JFCs are consistent with each other. The conversion efficiency from C_2H_2 to C_2H_6 is considered to be related to formation temperatures of these molecules. From the viewpoint of the nuclear spin temperature of water, which is thought to be the formation temperature of the species, typical OCs have ~30 K of the spin temperatures of water while SW3-B and C have >45 K of the water spin temperatures (Bockelée-Morvan et al. 2004; Dello Russo et al. 2007). If we assume that C_2H_2, C_2H_6, and H_2O formed in the same environment, it is considered that C_2H_6 formed in the region at ~30 K (typical OCs) or higher (e.g., SW3). On the other hand, Hiraoka et al. (2000) reported the temperature dependence of hydrogen-addition reactions and that hydrogen-addition reactions occurred efficiently at ~10 K and the yield of C_2H_6 dropped off dramatically at higher than 20 K. The $C_2H_6/(C_2H_6+C_2H_2)$ ratio may not be sensitive in the temperature range where cometesimals formed (~30 K). In Paper II, we reported the spin temperatures of water and methane, and D/H ratio of methane. These results indicate slightly high temperatures for the molecular formation than the typical OCs. From both the $(C_2H_2+C_2H_6)/H_2O$ ratio and the Paper II results, the cometesimals in C/2004 Q2 might have formed relatively closer to the proto-Sun (i.e., in warmer region) in the solar nebula than the typical OCs.

To determine the formation region of C/2004 Q2 more specifically, we should consider both chemical evolution of pre-

Figure 4. $C_2H_6/(C_2H_6+C_2H_2)$ ratios in comets listed in Table 4. As we mentioned in caption of Figure 3, the conversion efficiency from C_2H_2 to C_2H_6 is related to the $C_2H_6/(C_2H_6+C_2H_2)$ ratio. If the conversion efficiency showed high value, the conversion might have occurred effectively. The solid line shows the averaged value of the $C_2H_6/(C_2H_6+C_2H_2)$ ratio and dashed lines indicate $\pm 3\sigma$ error bars of averaged value.

(A color version of this figure is available in the online journal.)

Table 4
$(C_2H_6+C_2H_2)/H_2O$ and C_2H_6/C_2H_2 Ratios in Comets.[a]

$H_2O = 100$	$(C_2H_6+C_2H_2)/H_2O$ (%)	$C_2H_6/(C_2H_6+C_2H_2)$ (%)	Remarks
C/2004 Q2	0.5 ± 0.1	0.9 ± 0.2	This work
C/1996 B2	0.8 ± 0.1	0.8 ± 0.1	DiSanti & Mumma (2008)
C/1995 O1	0.9 ± 0.1	0.6 ± 0.1	DiSanti & Mumma (2008)
C/1999 H1	0.9 ± 0.1	0.7 ± 0.1	DiSanti & Mumma (2008)
153P/I-Z	0.8 ± 0.2	0.8 ± 0.3	DiSanti & Mumma (2008)
C/2001 A2	2.2 ± 0.2	0.8 ± 0.1	DiSanti & Mumma (2008)
1P/Halley	~ 0.7	~ 0.6	DiSanti & Mumma (2008)
C/1999 S4	< 0.23	> 0.5	DiSanti & Mumma (2008)
9P/Tempel 1	0.5 ± 0.1	0.8 ± 0.1	Post impact, DiSanti & Mumma (2008)
73P/SW3-B	0.19 ± 0.02	0.8 ± 0.2	Dello Russo et al. (2007), 2006 May 14.6
73P/SW3-C	0.16 ± 0.02	0.7 ± 0.1	Dello Russo et al. (2007), 2006 May 14.6

Note. [a] Error bars correspond to $\pm 1\tilde{\sigma}$. The lower limits correspond to 3σ limits.

cometary materials and dynamical evolution of planetesimals in the solar nebula. According to the "Nice model" (dynamical-evolutional model of planetesimals: Morbidelli et al. 2008), planetesimals were not formed in the region further than ~ 30 AU from the proto-Sun, and OCs were formed in the region from 5 to 30 AU in the solar nebula. So we can think that the further limit of the region where C/2004 Q2 formed is 30 AU. According to Aikawa et al. (1999), a chemical-evolutional model in the solar nebula, although the abundance ratios of HCN and CH_4 ices relative to H_2O ice are almost constant from 10– to 30 AU, the abundance ratio of C_2H_2 ice to H_2O ice is decreased dramatically in 25–30 AU. However, we note that Aikawa et al. (1999) did not take the grain surface chemistry into their model except the reactions forming H_2 molecules and recombination of electrons with ions on grains. Dodson-Robinson et al. (2009) also reported the chemical-evolutional model including the grain surface chemistry and there is no C_2H_2 ice depletion region around 25–30 AU in their result. Moreover, their result indicated that C_2H_2 ice is decreased dramatically within ~ 5 AU (at 1.5×10^6 yr). Their results are consistent with the hypothesis that comets 73P/SW3 and C/1999 S4 (LINEAR) known as "organic

depleted comets" formed ~ 5 AU (Mumma et al. 2001a; Dello Russo et al. 2007; Kobayashi et al. 2007). In the case of C/2004 Q2, C_2H_2 was depleted as 73P/SW3 whereas CH_4 was normal abundance, hence the formation region of C/2004 Q2 was not the same as 73P/SW3 (~ 5 AU) but slightly further away form the proto-Sun. We need more sophisticated chemical-evolution model in the solar nebula to determine the formation regions of cometesimals more precisely (e.g., Dodson-Robinson et al.'s calculation showed higher abundance of CH_4 than the typical cometary value).

Finally, we should mention that the $C_2H_6/(C_2H_6+C_2H_2)$ ratio depends on the period from the formation of icy grains to the incorporation of the grains into planetesimals in the solar nebula. The planetesimals aggregated each other and had grown into a comet in the solar nebula. Therefore, the chemical properties of planetesimals are related to the chemical properties of icy grains that the planetesimals originated in. Although the $C_2H_6/(C_2H_6+C_2H_2)$ ratio depends on the hydrogenation conditions, more H-atoms could stick on the surface of elder grains (that spent longer time in the solar nebula) than younger grains (that spent shorter time) if the H-atom density and the temperature

were constant through the time. Consequentially, the $C_2H_6/(C_2H_6+C_2H_2)$ ratio can vary with the period of icy grains. There is a report on the formation epoch of pre-cometary ices in comets 73P/SW3 and 9P/Tempel 1 (Villanueva et al. 2006). It was suggested that both 73P/SW3 and 9P/Tempel 1 may both have formed further than 5–10 AU from the Sun, but that 73P/SW3 formed later in time, after significant nebular clearing had allowed penetration of ionizing flux (producing higher H-atom densities) to greater distances with commensurate increasing processing of its pre-cometary ices. The relations between formation region and formation epoch of planetesimals and/or icy grains should be studied precisely in the future.

5. CONCLUSION

We performed high-dispersion spectroscopic observations of comet C/2004 Q2 (Machholz) in late 2005 January by using Keck II/NIRSPEC. We detected emission lines of H_2O, HCN, C_2H_2, NH_3, C_2H_4, C_2H_6, CH_3OH, and H_2CO in cometary spectra. The rotational temperature was determined as ~80 K from H_2O, HCN, and C_2H_2. We determined the mixing ratios of detected volatiles relative to water. We found that the mixing ratios of C_2H_2 and C_2H_6 in C/2004 Q2 were depleted compared with that of typical Oort Cloud comets while the mixing ratios of other volatiles (HCN, CH_4, CH_3OH, and H_2CO) were similar to that of typical OCs. We assumed the cometary nucleus of C/2004 Q2 was homogeneous and we discussed the formation conditions of icy planetesimals of C/2004 Q2 based on $(C_2H_6+C_2H_2)/H_2O$ and $C_2H_6/(C_2H_6+C_2H_2)$ ratios. From these ratios, we found that C/2004 Q2 formed in the region where the initial abundance of C_2H_2 was depleted and the conversion efficiency from C_2H_2 to C_2H_6 was comparable with other comets. However, the $C_2H_6/(C_2H_6+C_2H_2)$ ratio may not be sensitive in the temperature range where cometesimals formed (~30 K). To determine the formation region of C/2004 Q2 concretely, we employed the dynamical-evolutional model (the "Nice" model) and the chemical-evolutional model in the solar nebula. Based on the models, we found that C/2004 Q2 might have formed in inner region of the solar nebula, slightly further than 5 AU from the proto-Sun. This conclusion is supported by the result shown in Paper II (results of spin temperatures of CH_4 and H_2O, and D/H ratio of methane). We note that our observational results could be explained by the different formation periods of planetesimals in the solar nebula.

REFERENCES

A'Hearn, M. F., Millis, R. L., Schleicher, D. G., Osip, D. J., & Birch, P. V. 1995, Icarus, 118, 223
A'Hearn, M. F., et al. 2005, Science, 310, 258
Aikawa, Y., Umebayashi, T., Nakano, T., & Miyama, S. M. 1999, ApJ, 519, 705
Biver, N., et al. 1999a, AJ, 118, 1850
Biver, N., et al. 1999b, Earth Moon and Planets, 78, 5
Biver, N., et al. 2005, in IAU Symp. 229, Asteroids Comets Meteors, ed. D. Lazzaro, S. Ferraz-Mello, & J. A. Fernandez (Cambridge: Cambridge Univ. Press), 7

Biver, N., et al. 2008, Asteroids, Comets, Meteors (League City, TX: LPI), http://www.lpi.usra.edu/meetings/acm2008/pdf/8149.pdf
Bockelée-Morvan, D., Brooke, T. Y., & Crovisier, J. 1995, Icarus, 116, 18
Bockelée-Morvan, D., Crovisier, J., Despois, D., Forveille, T., Gérard, E., Schraml, J., & Thum, C. 1987, A&A, 180, 253
Bockelée-Morvan, D., Crovisier, J., Mumma, M. J., & Weaver, H. A. 2004, in Comets II, ed. M. C. Festou, H. U. Keller, & H. A. Weaver (Tucson, AZ: Univ. Arizona Press), 391
Bonev, B. P., Mumma, M. J., Gibb, E. L., DiSanti, M. A., Villanueva, G. L., Magee-Sauer, K.,, & Ellis, R. S. 2009, ApJ, in press
Bonev, B. P., Mumma, M. J., Villanueva, G. L., DiSanti, M. A., Ellis, R. S., Magee-Sauer, K., & Dello Russo, N. 2007, ApJ, 661, L97
Brooke, T. Y., et al. 2003, Icarus, 166, 167
Clough, S. A., Shephard, M. W., Mlawer, E. J., Delamere, J. S., Iacono, M. J., Cady-Pereira, K., Boukabara, S., & Brown, P. D. 2005, J. Quant. Spectrosc. Radiat. Transfer, 91, 233
Crovisier, J. 2007, Proc. 18th Rencontres de Blois: Planetary Science: Challenges and Discoveries, in press (arXiv:astro-ph/0703785)
Dello Russo, N., Bonev, B. P., DiSanti, M. A., Mumma, M. J., Gibb, E. L., Magee-Sauer, K., Barber, R. J., & Tnnyson, J. 2005, ApJ, 621, 537
Dello Russo, N., DiSanti, M. A., Magee-Sauer, K., Gibb, E. L., & Mumma, M. J. 2002b, Asteroids, Comets, Meteors (ESA SP-500, ESTEC; Noordwijk: ESA), 689
Dello Russo, N., DiSanti, M. A., Magee-Sauer, K., Gibb, E. L., Mumma, M. J., Barber, R. J., & Tennuson, J. 2004, Icarus, 168, 186
Dello Russo, N., Mumma, M. J., DiSanti, M. A., & Magee-Sauer, K. 2002a, J. Geophys. Res., 107, 5095
Dello Russo, N., Mumma, M. J., DiSanti, M. A., Magee-Sauer, K., Gibb, E. L., Bonev, B. P., McLeas, I. S., & Xu, L.-H 2006, Icarus, 184, 255
Dello Russo, N., Mumma, M. J., DiSanti, M. A., Magee-Sauer, K., & Novak, R. 2001, Icarus, 153, 162
Dello Russo, N., Vervack, R. J., Weaver, H. A., Biver, N., Bockelée-Morvan, D., Crovisier, J., & Lisse, C. M. 2007, Nature, 448, 172
Dello Russo, N., Vervack, R. J., Weaver, H. A., Montgomery, M. M., Desphande, R., Fernández, Y. R., & Martin, E. L. 2008, ApJ, 680, 793
Despois, D., Crovisier, J., Bockelée-Morvan, D., Schraml, J., Forveille, T., & Gérard, E. 1986, A&A, 160, L11
DiSanti, M. A., Dello Russo, N., Magee-Sauer, K., Gibb, E. L., Reuter, D. C., & Mumma, M. J. 2001, Asteroids, Comets, Meteors (ESA SP-500, ESTEC; Noordwijk: ESA), 571
DiSanti, M. A., & Mumma, M. J. 2008, Space. Sci. Rev., 138, 127
DiSanti, M. A., Villanueva, G. L., Bonev, B. P., Magee-Sauer, K., Lyke, J. E., & Mumma, M. J. 2007, Icarus, 187, 240
Dodson-Robinson, S. E., Willacy, K., Bodenheimer, P., Turner, N. J., & Beichman, C. A. 2009, Icarus, 200, 672
Duncan, M. J. 2008, Space. Sci. Rev., 138, 209
Eberhardt, P. 1999, Space, Sci. Rev., 90, 45
Eberhardt, P., Meier, R., Krankowsky, D., & Hodges, R. R. 1994, A&A, 288, 315
Farnham, T. L., Schleicher, D. G., Woodney, L. M., Birch, P. V., Eberhardy, C. A., & Levy, L. 2001, Science, 292, 1348
Feaga, L. M., A'Hearn, M. F., Sunshine, J. M., Groussin, O., & Farnham, T. L. 2007, Icarus, 191, 134
Fink, U. 2009, Icarus, 201, 311
Gibb, E. L., DiSanti, M. A., Magee-Sauer, K., Dello Russo, N., Bonev, B. P., & Mumma, M. J. 2007, Icarus, 188, 224
Gibb, E. L., Mumma, M. J., Dello Russo, N., DiSanti, M. A., & Magee-Sauer, K. 2003, Icarus, 165, 391
Hiraoka, K., Takayama, T., Euchi, A., Handa, H.,, & Sato, T. 2000, ApJ, 532, 1029
Huebner, W. F., Keady, J. J., & Lyon, S. P. 1992, Ap&SS , 195, 1
Kanda, Y., Mori, A., Kobayashi, H., & Kawakita, H. 2008, PASJ, 60, 1191
Kawakita, H., & Kobayashi, H. 2009, ApJ, 693, 388
Kobayashi, H., Kawakita, H., Mumma, M. J., Bonev, P. B., Watanabe, J., & Fuse, T. 2007, ApJ, 668, L75
Kurucz, R. L. 1994, in Proc. IAU Symp. 154, Synthetic Infrared Spectra, ed. D. M. Rabin, J. T. Jefferies, & C. Lindsey (Dordrecht: Kluwer), 523
Kurucz, R. L. 2005, Mem. Soc. Astron. Ital. Suppl., 8, 189
Lis, D. C., Bockelée-Morvan, D., Boissier, J., Crovisier, J., Biver, N., & Charnley, S. B. 2008, ApJ, 675, 931
Levison, H. F. 1996, in ASP Conf. Ser. 107, Completing the Inventory of the Solar System, ed. T. Retting & J. M. Hahn (San Francisco, CA: ASP), 173
Magee-Sauer, K., Dello Russo, N., DiSanti, M. A., Gibb, E. L., & Mumma, M. J. 2002a, Asteroids, Comets, Meteors (ESA SP-500, ESTEC; Noordwijk: ESA), 549
Magee-Sauer, K., Mumma, M. J., DiSanti, M. A., & Dello Russo, N. 2001, DPS meeting, #33, #20.09

Magee-Sauer, K., Mumma, M. J., DiSanti, M. A., & Dello Russo, N. 2002b, J. Geophys. Res., 107, 5096

Magee-Sauer, K., Mumma, M. J., DiSanti, M. A., Dello Russo, N., Gibb, E. L., & Bonev, B. P. 2008, Icarus, 194, 347

Magee-Sauer, K., Mumma, M. J., DiSanti, M. A., Dello Russo, N., & Rettig, T. W. 1999, Icarus, 142, 498

Marsden, B. G. 2004, M.P.E.C., 2004-U31

McLean, I. S., et al. 1998, Proc. SPIE, 3354, 566

Morbidelli, A., Levison, H. F., & Gomes, R. 2008, in The Solar System Beyond Neptune, ed. M. A. Barucci et al. (Tucson, AZ: Univ. Arizona Press), 275

Mumma, M. J., DiSanti, M. A., Dello Russo, N., Fomenkova, M., Magee-Sauer, K., Kaminski, C. F., & Xie, D. X. 1996, Science, 194, 347

Mumma, M. J., DiSanti, M. A., Dello Russo, N., Magee-Sauer, K., Gibb, E., & Novak, R. 2003, Adv. Space Res., 31, 2563

Mumma, M. J., et al. 2001a, Science, 292, 1334

Mumma, M. J., et al. 2001b, ApJ, 546, 1183

Mumma, M. J., et al. 2005, Science, 310, 270

Reuter, D. C., Mumma, M. J., & Nadler, S. 1989, ApJ, 341, 1045

Rothman, L. S., et al. 2005, J. Quant. Spectrosc. Radiat. Transfer, 96, 139

Schleicher, D. G. 2006, Cent. Bur. Electron. Tel., 491, 1

Schloerb, F. P., Kinzel, W. M., Swade, D. A., & Irvine, W. M. 1986, ApJ, 310, L55

Turner, N. J., & Smith, G. H. 1999, AJ, 118, 3039

Villanueva, G. L., Bonev, B. P., Mumma, M. J., Magee-Sauer, K., DiSanti, M. A., Salyk, C., & Blake, G. A. 2006, ApJ, 650, L87

Weaver, H. A., Brooke, T. Y., Chin, G., Kim, S. J., Bockelée-Morvan, D., & Davis, J. K. 1999, Earth Moon Planets, 78, 71